Numerical Investigation of Supersonic and Hypersonic Flows over a Flat Plate using a Thermally Perfect Gas Model

Neerav Krishna[1], Biswadip Shome[2]

[1]Neerav Krishna, BITS Pilani, Pilani Campus, f20230416@pilani.bits-pilani.ac.in

[2]Biswadip Shome, BITS Pilani, Pilani Campus, biswadip.shome@pilani.bits-pilani.ac.in

Abstract

High-speed external flows with free-stream Mach numbers exceeding 4-5 (M_∞ > 4-5) exhibit strong shock waves, steep temperature gradients, and molecular vibrational effects, leading to the breakdown of the calorically perfect gas assumption. This work investigates supersonic and hypersonic flow over a flat plate geometry to isolate and understand the physics under such conditions. An in-house Computational Fluid Dynamics (CFD) solver, implemented in Python and based on the MacCormack explicit finite-difference scheme, was developed for this purpose. The solver models a thermally perfect gas, incorporating temperature-dependent specific heats using two widely referenced formulations from the literature, namely, a polynomial functional form and an exponential functional form that is based on quantum theory. Comparative simulations using a calorically perfect gas model are performed to quantify the effect of incorporating a thermally perfect gas model. Viscosity is evaluated using Sutherland's law, while thermal conductivity is obtained from a constant molecular Prandtl number assumption. Near-wall resolution is achieved through y+ based meshing strategies, ensuring accurate boundary-layer characterization, and a mesh sensitivity study was performed to confirm grid independence of the results.

Analysis of predicted pressure, temperature, density, and Mach number distribution is done across both the calorically perfect gas and thermally perfect gas models. The influence of specific heat formulations on boundary-layer development and thermal gradients is systematically evaluated. The results demonstrate the necessity of temperature-dependent thermodynamic modelling to accurately predict the thermal and aerodynamic characteristics of high-speed flows. The insights obtained are directly applicable to the preliminary design of hypersonic vehicles, including missiles and high-speed aircraft. Possible extensions to this work can include the incorporation of automated mesh generation and the adaptation of the solver to handle blunt bodies, wedges, and lifting surfaces under high-speed flow conditions.

Key Words: *Computational Fluid Dynamics, Thermally Perfect Gas, Hypersonic Flow*

1) Introduction

Investigating flows over various geometries using Computational Fluid Dynamics (CFD) techniques is crucial for understanding, evaluating, and quantifying the physics of air flow in real-world applications. Using CFD unlocks the ability to analyse a broad range of setups in applications ranging from aircraft wings to cooling electronic devices to predicting weather. CFD also provides a quick, cost-effective, and adaptable method to carry out studies related to fluid flows, as a virtual environment enables rapid changes in code to simulate a new environment. And therefore, it acts as a great tool to build initial understanding and narrow down designs before a physical prototyping stage is reached. Thus, it is ideal to leverage these strengths of CFD techniques to simulate and understand physics in harsh environments such as those encountered in hypersonic flows.

A flat plate, being an elementary geometry, provides great insight and ease of comparison between multiple Gas models and flow regimes. Understanding the changes in key factors, such as temperature and pressure, and their distributions above the flat plate, provides the basis for designing more complex geometries and their applications in the Aerospace field. Koirala et al. [1] studied the distribution of pressure and temperature of a supersonic flow over a flat plate using a Calorically Perfect Gas (CPG) model. The study showed a common underlying pattern in the temperature and pressure distributions of the boundary layer across different free-stream velocities, with peak temperatures at the trailing edge of the flow reaching approximately 580 K for $M_\infty = 5.2$. A study by Tatum [2] reveals that once temperatures above 500 K are reached, air molecules begin to store energy in vibrational modes, leading to a variation in the value of specific heat (c_p) as a function of only temperature until dissociation starts around 1500 K. This specific heat behaviour which depends on temperature only is commonly referred to as a Thermally Perfect Gas (TPG) model. The study further provides a polynomial relationship for the TPG model. A report by NACA [3] delves into modelling a diatomic gas as a simple harmonic oscillator to quantify the energy stored in the vibrational mode that leads to an increase in the specific heat value. This model, which is common and easy to use, is often referred to as the s the Exponential form of the TPG model. Studies such as those by Toro et al. [4] and by Vetlutskii et al. [5] have investigated hypersonic flows over a flat plate but were limited to using a CPG model that leads to deviations in comparison to more realistic TPG models.

The objective of this study is to establish a clear comparison of temperature and pressure distributions in the boundary layers of the flow between the 3 aforementioned models, i.e., the CPG model, the TPG model using a polynomial function, and the TPG model using an exponential function. The comparison is done across a range of free-stream velocities ranging from $M_\infty = 2$ to $M_\infty = 10$ over a constant temperature flat plate setup. This study provides a novel approach by developing a CFD solver written in Python based on the 2nd order MacCormack technique using NumPy, SciPy, and Matplotlib [6]. This results in a clearly quantified and concrete difference between the models for a simple geometry, which can further be used to analyze complex geometries for high speed applications.

2) Governing Equations and Numerical Methods

2.1 Governing Equations

The two-dimensional Navier-Stokes equations of mass conservation, momentum conservation, and energy conservation, along with assumptions for equation closure, are used to solve for this hypersonic flow over a flat plate problem. The time transient conservation equations in Cartesian coordinates are:

Mass conservation: $\frac{\partial \rho}{\partial t} + \frac{\partial(\rho u)}{\partial x} + \frac{\partial(\rho v)}{\partial y} = 0$ (1)

Momentum conservation in the x-direction: $\frac{\partial(\rho u)}{\partial t} + \frac{\partial(\rho u^2 + p - \tau_{xx})}{\partial x} + \frac{\partial(\rho u - \tau_{yx})}{\partial y} = 0$ (2)

Momentum conservation in the y-direction: $\frac{\partial(\rho v)}{\partial t} + \frac{\partial(\rho v^2 + p - \tau_{yy})}{\partial y} + \frac{\partial(\rho u - \tau_{yx})}{\partial x} = 0$ (3)

Energy equation conservation: $\frac{\partial E_t}{\partial t} + \frac{\partial((E_t + p)u + q_x - u\tau_{xx} - v\tau_{xy})}{\partial x} + \frac{\partial((E_t + p)v + q_y - u\tau_{xy} - v\tau_{yy})}{\partial y} = 0$ (4)

where, $E_t = \rho\left(e + \frac{V^2}{2}\right)$

2.2 Assumptions

The assumptions made for the closure of the two-dimensional Navier-Stokes equations are as follows:

1) Ideal Gas Law: $P = \rho RT$
2) Sutherland's Law: Used to calculate temperature-dependent viscosity$\mu = \mu_0 \left(\frac{T}{T_0}\right)^{3/2} \frac{T_0+110}{T+110}$
3) Constant value of Prandtl number of Pr $\frac{\mu c_p}{k} = 0.71$
4) Specific heat Models: C_p-T obtained using either CPG model, exponential form of TPG model (Exp-TPG), or the polynomial form of the-TPG model (poly-TPG)

a. $C_p = \text{constant}$ CPG

b. $$C_p = \left(C_p\right)_{perf}\left\{1+\frac{\gamma_{perf}-1}{\gamma_{perf}}\left[\left(\frac{\theta}{T}\right)^2 \frac{e^{\theta/T}}{(e^{\theta/T})^2}\right]\right\}$$ Exp-TPG

c. $C_p = a_0T^{-2} + a_1T^{-1}+a_2 + a_3T + a_4T^2 + a_5T^3 + a_6T^4 + a_7T^5$ Poly-TPG

Using these assumptions, we can formulate a closed set of equations that can be then solved using the second-order accurate MacCormack scheme [6] technique to arrive at a solution.

2.3 MacCormack Subroutine

The MacCormack scheme advances the solution in time using a two-step predictor-corrector approach. This provides a second-order accurate solution while maintaining linearity in the numerical method. The steps involve

Predictor Step (Forward Differencing): $U_i^* = U_i^n - \frac{\Delta t}{\Delta x}(F_{i+1}^n - F_i^n) + \Delta t S_i^n$

Corrector Step (Backward Differencing): $U_i^{n+1} = \frac{1}{2}\left[U_i^* + U_i^n - \frac{\Delta t}{\Delta x}(F_{i+1}^* - F_i^*) + \Delta t S_i^*\right]$

Where, U_i^* is the computed provisional solution, $U = \begin{bmatrix}\rho\\ \rho u\\ \rho E\end{bmatrix}$ & $F = \begin{bmatrix}\rho u\\ \rho u^2+p\\ u(\rho E+p)\end{bmatrix}$

2.4 Geometry and Grid Independence Test

For computational simplicity and property comparison across free-stream Mach numbers, the Reynolds number at the trailing edge was maintained at $Re = 400$. The freestream pressure and temperature were assumed to be 1 atm and 283 K, respectively

The height of the computational domain was assumed to be 5 times the laminar boundary layer height as predicted by the Blasius solution [6]. As stated in [6], the magnitude of Reynolds' number across a grid cell was used as a basis to determine the grid density. Maintaining $Re_{\Delta x} \leq 30 \text{ and } Re_{\Delta y} \leq 3$ provides a baseline to run the grid independence test. For computational simplicity, the CPG model with a freestream Mach 5 condition was chosen for performing the grid sensitivity tests. The grid sensitivity tests were run for 5 grid densities ranging from 40 x 120 to 60 x 160. To quantify the differences produced due to the grid, the maximum temperature observed in the flow was chosen as the comparison metric. It was observed that after a grid density of 50 x 140 cells, no change in the metric was observed. Therefore, a 50 x 140 grid was chosen for all subsequent cases in this work.

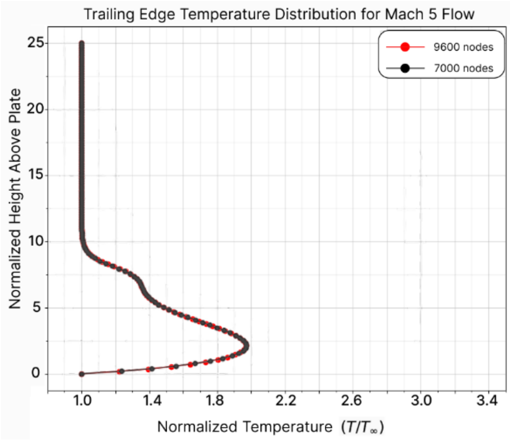

Grid	Maximum Temperature (K)
40 x 120	599.32
50 x 140	604.53
60 x 160	604.61

Figure 1 Grid Independence Test Result Comparison **Table 1 Grid Independence Test Results**

2.5 Solver Validation

The results obtained from the in-house solver were compared to the results in [7]. Using the maximum value of temperature at the trailing edge as a quantifiable comparison metric across free-stream velocities ranging from Mach 2 to Mach 5, a maximum of 3.5% error was observed. The small difference observed between the present results and previously published results serves as a validation of the present methodology

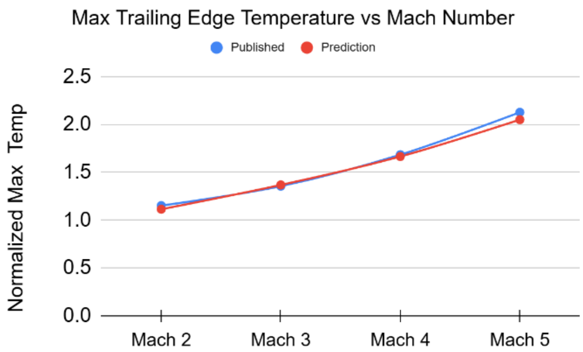

Figure 2 Solver Validation Cases

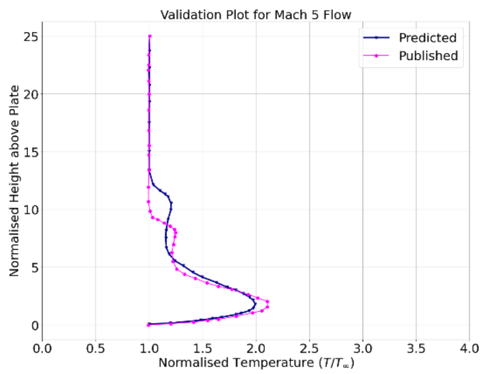

Figure 3 Mach 5 Flow Trailing Edge Temperature Profile Comparison

3) Results and Discussion

This section presents the key outcomes of the present study, focusing on shock layer characteristics, temperature and pressure distributions, and comparative performance of the different models across a wide range of Mach numbers.

3.1 Shock Layer

The variation of shock layer height with Reynolds number for Mach numbers ranging from 2 to 10 is shown in Fig. 4. For a fixed value of Reynolds number, the shock height decreases significantly with increasing Mach number. Quantitatively, the shock height at Mach 2 is approximately twice that observed at Mach 5 and nearly three times that at Mach 10 for the same Reynolds number. To capture the observed trends, a quadratic polynomial regression was employed to fit the shock height as a function of Reynolds number for each Mach number. The quadratic model provided an excellent fit across the entire Reynolds number range.

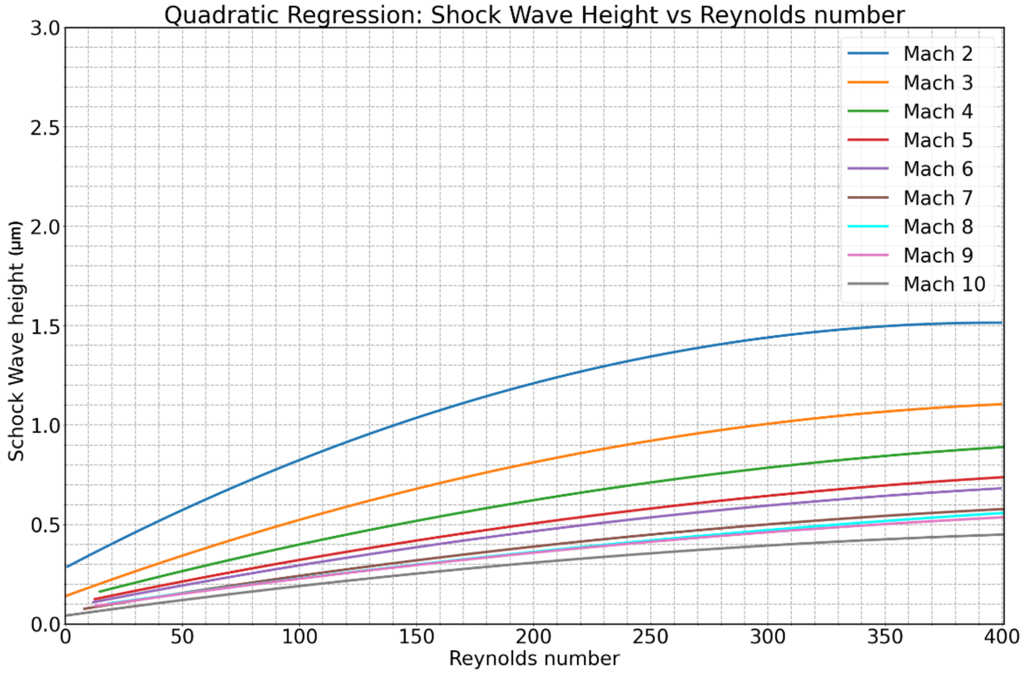

Figure 4 Quadratic Curves for Shock Layers

Table 2 Equations of Quadratic Polynomial Fit

Mach Number	a (coefficient of x^2)	b (coefficient of x)	c (intercept)
2	-7.796375×10^{-6}	6.201520×10^{-3}	2.817222×10^{-1}
5	-2.255655×10^{-6}	2.513773×10^{-3}	9.278200×10^{-1}
7	-1.756365×10^{-6}	1.996906×10^{-3}	5.953531×10^{-1}
10	-1.567384×10^{-6}	1.646432×10^{-3}	4.119507×10^{-1}

3.2 Pressure and Temperature Distributions

Representative temperature and pressure contours for various flows are shown in Fig. 5 and Fig. 6. The pressure contour shows a sharp gradient across the shock, followed by a decay toward the wall, consistent with strong compression effects typical of hypersonic flows.

Similarly, the temperature distribution displays a thermal layer bounded by the shock. Peak temperatures are observed near the wall due to strong compression. The shock layer thickness inferred from both pressure and temperature contours is consistent with the shock height trends discussed earlier, lending confidence to the overall predictions. Fig. 8 presents a comprehensive comparison of trailing edge temperature distribution across Mach numbers.

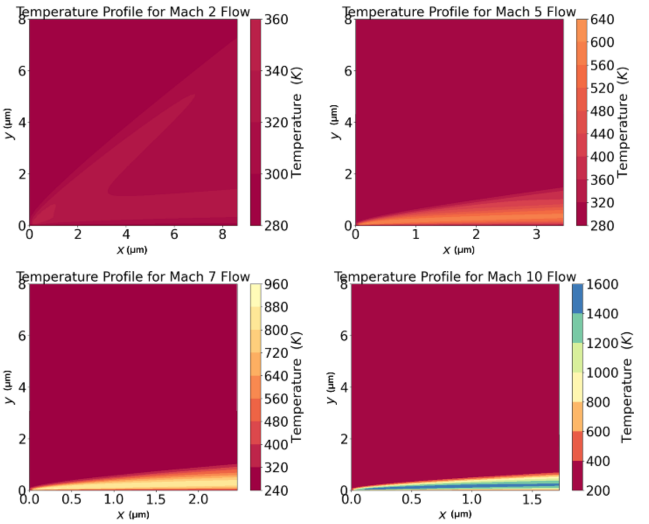

Figure 5 Temperature Contours for Various Free Stream Velocities

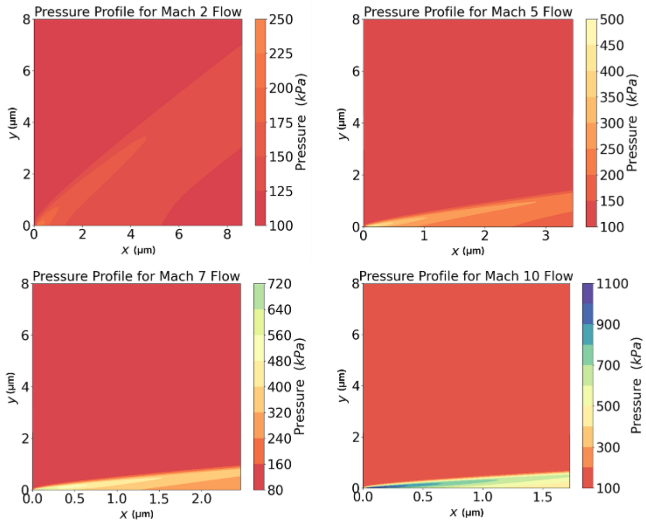

Figure 6 Pressure Contours for Various Free Stream Velocities

3.3 Comparison Between CPG and TPG Models

A detailed comparison between the CPG model and the TPG polynomial model was performed to assess the impact of temperature-dependent gas properties on predicted flow quantities. Trailing-edge temperature and pressure distributions are shown in Fig. 7.

The maximum deviation in temperature between the CPG and TPG exponential models was found to be approximately 130 K, occurring near the peak of the thermal boundary layer. This difference highlights the increasing importance of variable gas properties at high Mach numbers, where temperature gradients are large. In contrast, the deviation in maximum pressure between the two models was limited to approximately 40 kPa, indicating that pressure predictions are comparatively less sensitive to temperature-dependent properties under the present conditions.

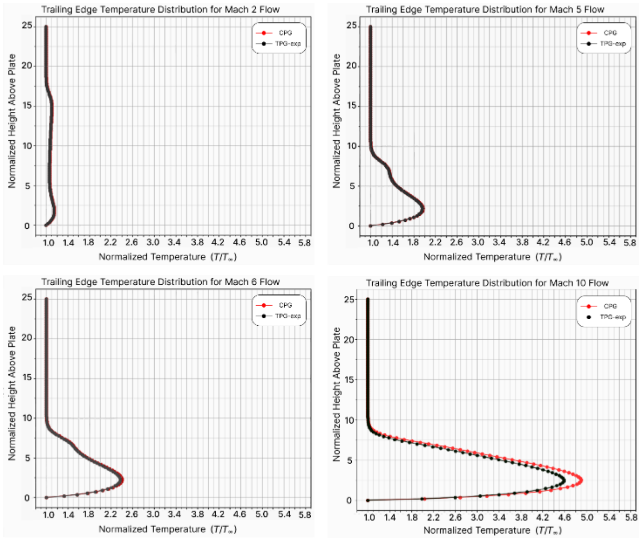

Figure 7 Comparison of CPG and TPG Models

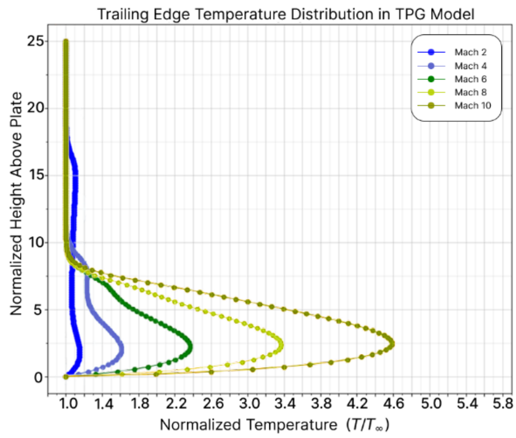

Figure 8 Trailing Edge Temperature Distributions of Various Free Stream Velocities

Notably, the predicted shock layer heights from the CPG and TPG models were found to be identical. This suggests that, while thermodynamic property variation significantly affects temperature levels within the shock layer, the overall shock geometry is not affected significantly.

3.4 Polynomial vs Exponential TPG Model Comparison

To further evaluate modelling sensitivity, results from polynomial and exponential formulations of the TPG model were compared. The variation of maximum temperature with Mach number for CPG, TPG-polynomial, and TPG-exponential models is shown in Fig. 9.

The maximum temperature deviation between the polynomial and exponential TPG models was limited to 7 K across the entire Mach number range, demonstrating excellent agreement between the two formulations. Similarly, the maximum pressure deviation between the TPG models was found to be only 8 kPa, which is negligible relative to absolute pressure levels in hypersonic flow.

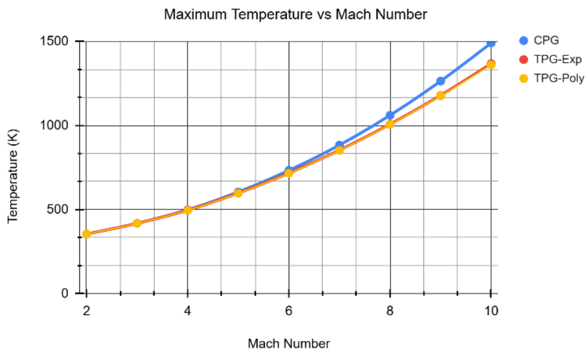

Mach Number	Maximum temperature (K)		
	CPG	Exp	Poly
2	354	354	354
5	604	597	596
10	1490	1367	1360

Figure 9 Variation of Maximum Flow Temperature (Left) Table 3 Maximum temperature vs Mach Number (Right)

4) Conclusions

In this study, the effects of Mach number and various gas models on shock layer characteristics and thermal predictions in high-speed compressible flow were systematically examined. The results show that the shock layer height is inversely proportional to the freestream Mach number, with increasing Mach number leading to progressively thinner shock layers due to stronger compressibility effects.

A detailed comparison between the calorically perfect gas (CPG) and two thermally perfect gas (TPG) models reveals that temperature predictions differ significantly at higher Mach numbers. At a freestream Mach number of 10, the maximum deviation between CPG and TPG temperature predictions was found to be as high as 9.7%, indicating that the constant specific heat assumption inherent to the CPG model becomes increasingly inaccurate in hypersonic regimes. At lower Mach numbers, these differences diminish, suggesting that the CPG assumption remains acceptable for low-to-moderate supersonic flows.

The performance of the exponential and polynomial formulations of the TPG model was also evaluated. Both approaches produced nearly identical results over the entire Mach number range considered, with maximum deviations limited to 0.5% even at Mach 10. This close agreement confirms the robustness of thermally perfect gas modelling for high-temperature flows. Among the two formulations, the exponential TPG model is preferable due to its smooth functional form, elimination of piecewise curve fitting, and ease of implementation in numerical solvers.

Observations also lead to the conclusion that, over a range of Mach numbers, the maximum temperature at the trailing edge of the flow is encountered at a height of 2.5 times the Blasius boundary layer height.

Overall, the results demonstrate that while CPG models may be sufficient for preliminary analyses at lower Mach numbers, accurate prediction of thermal fields in hypersonic flows requires the use of TPG models. The findings provide practical guidance for selecting appropriate gas property formulations in high-speed flow simulations and support the adoption of TPG-based approaches for reliable hypersonic aerodynamic and thermal analyses.

References

1. R. R. P. Koirala, K. V. S. Santosh Kumar, S. Adhikari, and D. Praveen, "Numerical simulation and analysis of supersonic flow over a flat plate," *IOSR Journal of Mechanical and Civil Engineering*, vol. 4, no. 6, pp. 36–41, Jan.–Feb. 2013. **DOI:** https://doi.org/10.9790/1684-0463641

2. K. E. Tatum, *Computation of thermally perfect properties of oblique shock waves*, NASA Langley Research Centre, Tech. Rep., 1996. Available: https://ntrs.nasa.gov/citations/19960050025

3. *Ames Research Staff, Equations, Tables, and Charts for Compressible Flow, NACA Rep. 1135, National Advisory Committee for Aeronautics, 1953. Available:* https://www.grc.nasa.gov/www/k-12/airplane/Images/naca1135.pdf

4. P. G. P. Toro, Z. Rusak, L. N. Myrabo, and H. T. Nagamatsu, "Hypersonic flow over a flat plate," *AIAA Paper* 98-0683, Jan. 1998. Available: https://arc.aiaa.org/doi/abs/10.2514/6.98-0683

5. *V. N. Vetlutskii, A. A. Maslov, S. G. Mironov, T. V. Poplavskaya, and A. N. Shiplyuk, "Hypersonic flow on a flat plate. Experimental results and numerical modeling," J. Appl. Mech. Tech. Phys., vol. 36, no. 6, pp. 848–854, 1995,* ***DOI:*** https://doi.org/10.1007/BF02369381

6. J. D. Anderson, Jr., *Computational Fluid Dynamics: The Basics With Applications*, McGraw-Hill, New York, NY, USA, 1995, ISBN: **978-0-07-001685-9**.

7. *D. Banos and D. Law, "Numerical simulation of a supersonic flow over a flat plate," in Proc. ASME Int. Mech. Eng. Congr. Expo. (IMECE), Portland, OR, USA, Nov. 2024, Paper IMECE2024-144710*. **DOI:** https://doi.org/10.1115/IMECE2024-144710